

Supplementary Information

Effects of Structurally – Related Impurities on the Crystal Growth of Curcumin Spherulites

Claire Heffernan¹, Rodrigo Soto^{1,2,}, Marko Ukrainczyk¹, Jacek Zeglinski¹, Benjamin K.
Hodnett¹, Åke C. Rasmuson^{1,3}*

¹*Synthesis and Solid State Pharmaceutical Centre (SSPC), Bernal Institute, Department of Chemical Sciences, University of Limerick. Limerick V94 T9PX, Ireland.*

²*Department of Chemical Engineering and Analytical Chemistry. University of Barcelona, Martí i Franqués 1-11, 08021 Barcelona, Spain.*

³*Department of Chemical Engineering and Technology, KTH Royal Institute of Technology, SE-100 44 Stockholm, Sweden.*

**Corresponding author email: r.soto@ub.edu*

S1. Materials and analysis of solid and liquid samples

Crude CUR (>75% HPLC) was purchased from Merck, containing <20% DMC and <5% BDMC. The material was separated and purified into fractions of CUR (100% HPLC), DMC (98.6% HPLC) and BDMC (98.3% HPLC) by cooling crystallization followed by column chromatography, as previously reported.¹ Propan-2-ol (IPA, $\geq 99.9\%$ purity) was purchased from VWR.

CUR seed were prepared and characterized by the method previously reported in our study of pure CUR in pure propan-2-ol.² The same seed CUR material (Form I) used in that study was used here for a consistent comparison of results. The crystal habit of the prepared CUR seed material is spherulites each made up of tiny needle shaped crystals. Because of brittleness, no sieving into a particular size fraction was done.

A Zeiss MCS651 spectrophotometer fitted with a Hellma 661.812 Attenuated Total Reflection (ATR) UV-Vis fiber optic immersion probe (supplied by Clairet Scientific, Northampton, UK) was used to measure the changes in the solution concentration of CUR by measuring the absorbance of CUR at 1 minute intervals. A spectral wavelength range used was 400–500 nm using Aspect plus software. The curcuminoids absorb in the UV–Visible range with λ_{max} at 425 nm.³ Focused beam reflectance measurement (FBRM, G400 particle track, Mettler-Toledo) was used to measure the chord length distributions (CLD) and to record the change in count number at a measurement interval of 10 s. The HPLC instrument and method used in the analysis of the collected crystal particles is the same as in previously published work.¹ Hitachi SU-70 Field Emission SEM without conductive coatings was used to observe the various CUR crystal products obtained in the absence and presence of impurities. As a result, a low primary electron beam energy (1 keV) was used for all image acquisitions in order to minimise specimen charging. All diffraction patterns were recorded on a PANalytical EMPYREAN diffractometer system using Bragg–Brentano geometry and an incident beam of Cu K-alpha radiation ($\lambda = 1.5406 \text{ \AA}$). Room temperature scans were performed on a spinning silicon sample holder (step size = $0.013^\circ 2\theta$ and step time = 32 (s)).

S2. PXRD data collected

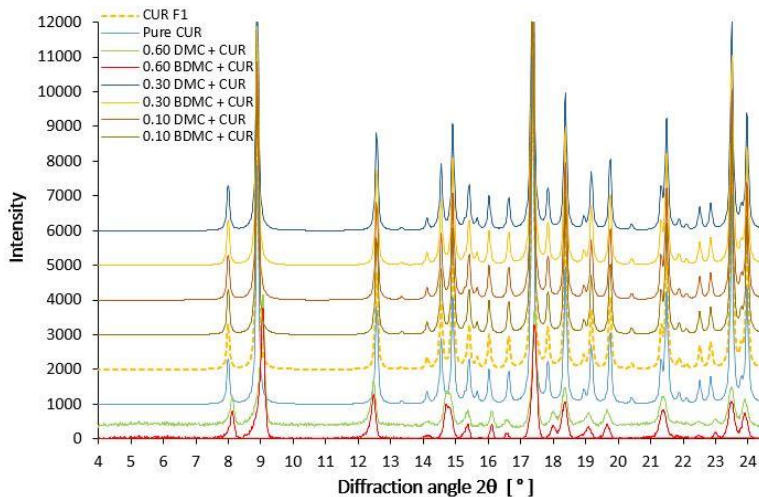


Figure S2. PXRD data of CUR Form I (BINMEQ04) and of CUR particles collected after growth in the presence of the indicated concentrations of impurities. $T_{\text{cryst}} = 308 \text{ K}$; Cu K- α $\lambda = 1.5406 \text{ \AA}$.

S3. Supersaturation dependence of the growth rate at different conditions

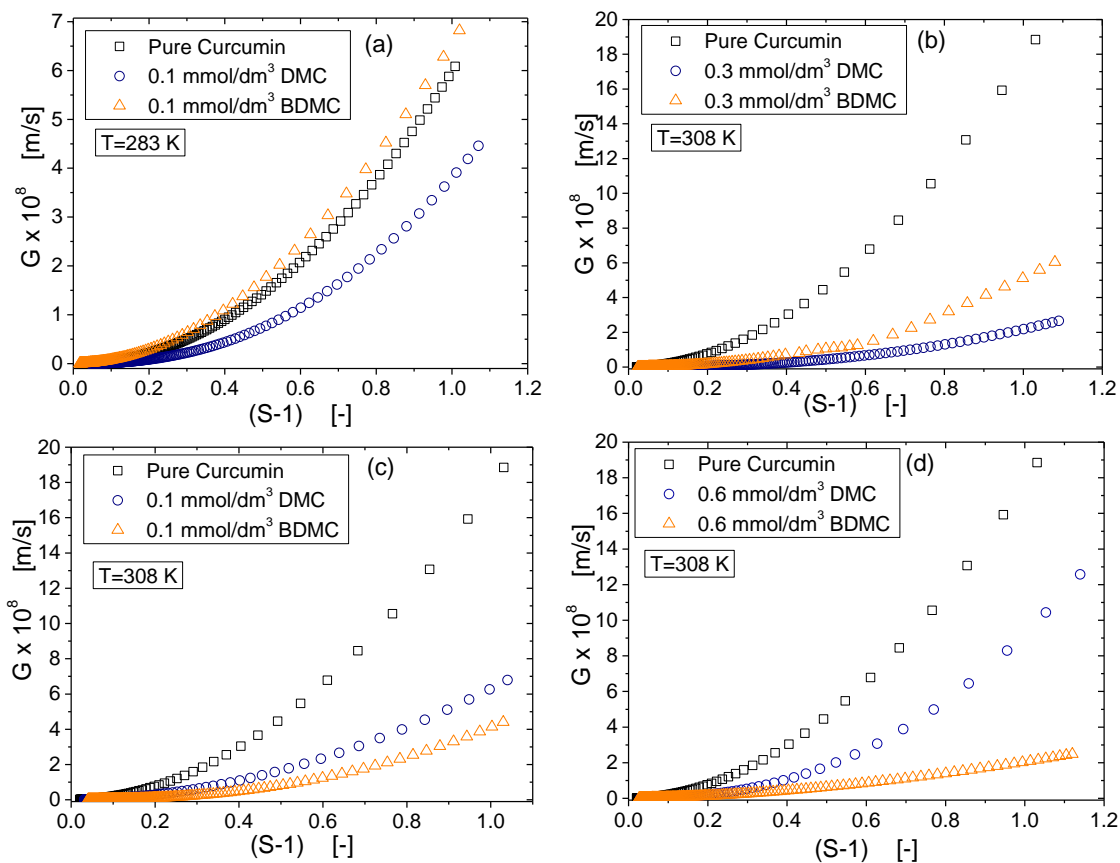


Figure S3. Comparison of estimated growth rates at different conditions from fitting of power law equation to experimental data in the absence and in the presence of DMC and BDMC.

S4. Molecular modelling

The solid solution thermodynamics quantities (enthalpy of mixing, ΔH_{mix} , entropy of mixing, ΔS_{mix} , and Gibbs free energy of mixing, ΔG_{mix}) are calculated based on a regular solution model upon BDMC substitution in the crystal lattice of CUR Form 1 at two different concentrations of the impurity: 2 mol% and 6 mol% (Table S1). The results show that while the incorporation of BDMC impurity into lattice of CUR is not favorable thermodynamically (positive values of ΔG_{mix}), the entropy of mixing stabilizes to some extent the unfavorable inclusion of the impurity, and higher the concentration of BDMC the more stabilization comes from the entropy term.

Table S4. Calculated lattice parameters and total energy of the simulated CUR supercells with varying BDMC composition as well as derived thermodynamics results.

x_{BDMC} (mol%)	Molecular supercell simulation				Solid-solution thermodynamics				
	a (Å)	b (Å)	c (Å)	E_{tot} (kJ/mol)	ΔS_{mix} (J/mol/K)*	$T\Delta S_{\text{mix}}$ (kJ/mol)	ΔH_{mix} (kJ/mol)	ΔG_{mix} (kJ/mol)**	
0	12.58	7.04	19.95	-221	0	0	0	0	
2	12.61	6.91	19.80	-219	0.81	0.24	1.13	0.89	
6	12.58	6.96	19.67	-220	1.88	0.56	1.29	0.73	

* ΔS_{mix} calculated based on ideal entropy of mixing, Eq. S1. ** ΔG_{mix} calculated based on regular solution model, Eq. S3

$$\Delta S_{\text{mix}} = -R(x \cdot \ln x + (1-x) \cdot \ln(1-x)) \quad (1)$$

$$\Delta H_{\text{mix}} = E_{\text{solid solution}} - x \cdot E_{\text{impurity}} - (1-x) \cdot E_{\text{CUR}} \quad (2)$$

$$\Delta G_{\text{mix}} = \Delta H_{\text{mix}} - T\Delta S_{\text{mix}} \quad (3)$$

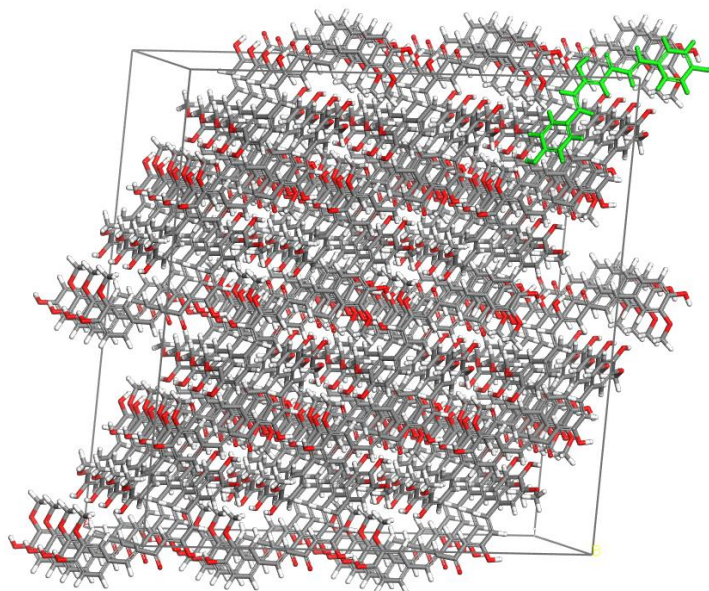


Figure S4. Constructed supercell (3x4x2) used for geometry optimisation calculations.

References

- 1 C. Heffernan, M. Ukrainczyk, R. K. Gamidi, B. K. Hodnett, Å. C. Rasmuson, *Org. Process Res. Dev.*, **2017**, 21, 821–826.
- 2 C. Heffernan, R. Soto, B. K. Hodnett, Å. C. Rasmuson, *CrystEngComm*, **2020**, 22, 3505-3518
- 3 K. I. Priyadarsini, *Molecules*, **2014**, 19, 20091–20112.